A1313

Processing and durability of fuel electrode supported-cells with Ni-GDC electrode

Christian Lenser (1), Denise Ramler (1,2), Stefan Kucharski (1), Luzie Wehner (3), Egbert Wessel (3), Jürgen Malzbender (3), Lukas Schöller (4), Daniel Schneider (4,5), Britta Nestler (4,5), Iurii Kogut (6), André Weber (6), Norbert H. Menzler (1,2)

(1) Institute of Energy Materials and Devices (IMD), Materials Synthesis and Processing (IMD-2), Forschungszentrum Jülich GmbH 52425 Jülich/Germany

(2) Institute for Mineral Engineering (GHI), RWTH Aachen University, Forckenbeckstr. 33, 52074 Aachen, Germany

(3) Institute of Energy Materials and Devices (IMD), Structure and Function of Materials (IMD-1), Forschungszentrum Jülich GmbH, 52425 Jülich/Germany

(4) Institute for Applied Materials (IAM-MMS), Karlsruhe Institute of Technology (KIT), Strasse am Forum 7, 76131 Karlsruhe, Germany

(5) Institute of Digital Materials Science (IDM), Karlsruhe University of Applied Sciences, Moltkestrasse 30, 76133 Karlsruhe, Germany

(6) Institute for Applied Materials (IAM-ET), Karlsruhe Institute of Technology (KIT), Adenauerring 20b, 76131 Karlsruhe, Germany

c.lenser@fz-juelich.de

Abstract

The incorporation of Ni-GDC electrodes into fuel-electrode supported cells (FESC) was investigated as a pathway to increase the durability of solid oxide electrolysis cells (SOEC). High-performance SOEC using a three-layer electrolyte made of ceria and zirconia layers were fabricated using both physical vapour deposition (PVD) and suspension-based processing techniques. In order to assess the mechanical limits of the cell due to electro-chemical-mechanical coupling during SOE operation, a 3-dimensional model was created using synthetic microstructures based on the parameters determined through 3-dimensional reconstructions of real cells. Information about the mechanical properties of the materials and the chemical expansion of GDC under cathodic potential were determined with dedicated experiments and used to model stresses in the system in dependence of microstructure and operation conditions.

In order to fabricate cells using suspension-based techniques, the screen-printing pastes and resulting microstructures were optimized. Based on a new understanding of the correlation between paste rheology and the properties of the printed layers, co-fired multi-layer electrolytes showed good adhesion and stability. However, it could be shown that interdiffusion during sintering is significantly enhanced during co-firing compared to sequential sintering, leading to short circuiting in the cells. A sequentially fired, multi-layer electrolyte was implemented that demonstrates the feasibility of Ni-GDC electrode in an FESC produced through common ceramic techniques. The main conclusions and lessons learned from the ElChFest project will conclude this contribution.

Introduction

The utilization of cermet cathodes made from Ni and Gd-doped ceria (GDC) for solid oxide electrolysis cells (SOEC) is well-established in electrolyte- and metal-supported cell designs.[1,2] However, their utilization is restricted in cathode-supported cells (CSC) designs due to processing issues associated with the high sintering temperature of the half-cell, leading to strongly reduced cell performance when co-sintering NiO-GDC with a yttria-stabilized zirconia (YSZ) electrolyte.[3] The performance loss is attributed to the reduced conductivity of the YSZ-GDC mixed phase that forms at the interface, as well as to the formation of porosity due to the difference in the diffusion coefficients of Gd^{3+} and Ce^{4+} in YSZ on the one hand, and Y^{3+} and Zr^{4+} in GDC on the other (Kirkendall effect).[4,5] Different strategies have been put forward to mitigate this issue, among them the reduction of sintering temperature of the half-cell,[6] or the introduction of a GDC layer adjacent to the NiO-GDC cathode.[7] While electronic leakage associated to single-layer ceria electrolytes is a manageable problem in fuel cell operation at low temperature,[8] the lowered oxygen activity associated to the cathode overpotential in an SOFC strongly increases electronic leakage in GDC and necessitates the use of an electron-blocking layer made from zirconia. This layer has to be protected from $SrZrO_3$ formation during anode sintering, leading to a three-layer GDC-YSZ-GDC electrolyte design.

There are few reports in the literature about the electrochemical performance and degradation behavior of CSC with Ni-GDC cathodes. Klitkou, Lopez de Moragas et al. report a fairly high resistance of approximately 0.8-0.9 Ωcm² at 750 °C in 90:10 H_2O:H_2, but good stability.[6] Improving on this, optimization of the cathode microstructure resulted in a reduced area-specific resistance of 0.46 Ωcm² under the same conditions.[9] These values are quite a bit higher than comparable data for state-of-the-art Ni-YSZ based cells, indicating that there is still potential for improvement.

1. Scientific Approach

In order to integrate Ni-GDC cathodes into CSCs, two different approaches were pursued. The first approach was to use a GDC electrolyte layer deposited by screen-printing and co-sintered with the NiO-GDC electrode on a NiO-YSZ support, followed by the deposition of a YSZ and a second GDC layer by reactive magnetron sputtering. This cell is called PVD-cell. The second approach is to co-sinter multiple screen-printed layers of GDC and YSZ to achieve a three-layered electrolyte without the use of PVD layers. This cell is labelled SP-cell.

While the manufactured cells had a size of 5x5 cm² in the sintered state, cell testing was performed using an active area of 1 cm² to avoid gradients in current density or gas conversion rate in the investigated electrode. Long-term stability was assessed in rather aggressive conditions at 800 °C, with a steam:hydrogen ratio of 1:1 and a current density of 1.5 Acm^{-2}.

Post-test analysis reveals the formation of vertical cracks in the GDC electrolyte layers. In the case of the PVD-cells, this correlates to a decrease in open circuit voltage during long-term testing, while the SP-cells show stable OCV but strong degradation, likely due to delamination between the GDC and YSZ electrolyte layer.

2. Experiments/Calculations/Simulations

The full description of experimental procedures and simulation approaches will be published elsewhere (currently under review).[10] Briefly, the cells were processed on a tape-cast NiO-YSZ support developed in-house.[11] NiO-GDC, GDC and YSZ screen-printing pastes were synthesized using NiO powder (Green NiO, Vogler, NL), GDC powder (10GDC-M, Fuelcellmaterials, USA) and YSZ powder (TZ-8Y, Tosoh, Japan) after pre-calcination and milling, mixed with α-terpineol and ethyl cellulose. Screen-printing was performed with a semi-automatic screen-printer (EKRA E2, EKRA Automatisierungssysteme GmbH, Germany). The half-cell, consisting of NiO-YSZ support, NiO-GDC cathode and either a single GDC layer (PVD-cell) or multiple GDC-YSZ-GDC layers, were sintered at 1400 °C for 5 hours in air. A second batch of cell were sintered with a GDC-YSZ bilayer, and an additional GDC layer was after half-cell sintering and sintered at 1300 °C. To achieve sufficient flatness for cell testing, the cells were subjected to a high-temperature forced creep deformation step at < 1400 °C where necessary. PVD-cells were then coated with a 0.5 µm thick layer of YSZ by reactive magnetron sputtering from a metallic Y-Zr target, followed by a GDC layer deposited in an equivalent manner. $La_{0.58}Sr_{0.4}CoO_{3-\delta}$ (LSC) or $La_{0.58}Sr_{0.4}Co_{0.2}Fe_{0.8}O_{3-\delta}$ (LSCF) air electrodes were deposited by screen-printing using in-house produced materials.

Electrochemical testing of the cells was performed in the temperature range of 600 – 800 °C, using dry laboratory air and a fuel gas stream composed of H_2 and varying amounts of H_2O (5-80%). The air-side and fuel-side contacting was performed using a Au- or Ni-mesh, respectively. Electrochemical impedance spectroscopy was performed using a Solartron SI1260 analyzer, and I-V characteristics were recorded using an Agilent 6612 DC power supply and an Agilent 34970A data acquisition unit.
Reference measurements were performed with CSC using Ni-YSZ and Ni(10%Fe)-YSZ cells provided by Forschungszentrum Jülich.

Microstructure reconstruction was performed with focused ion beam / scanning electron microscopy (FIB/SEM) analysis, using a Helios 5 CXe (Thermo Fischer Scientific, Hillsboro, USA). Reconstruction was performed using the Avizo software package.

3. Results

The full description of experimental and simulation results will be published elsewhere (currently under review).[10]
Co-sintering the GDC-YSZ-GDC at 1400 °C for 5 hours yields a mechanically stable trilayer electrolyte with thickness of approximately 12 µm. However, the open circuit voltage (OCV) of these cells is between 600 and 700 mV at 800 °C in dry H_2, as shown in Figure 1 with the black triangles. Increasing the YSZ layer thickness increases the OCV significantly to almost 1100 mV, but the cells show a very high resistance (black squares). Sintering a thinner YSZ layer as a bilayer with GDC, and then adding either a SP-GDC layer (blue squares) or a PVD-GDC layer (grey squares) results in an OCV above 1 V and a significantly reduced cell resistance. It must be stressed that the OCV is likely strongly influenced by the strong curvature of these cells, as that prevents the gold ring to effectively seal the setup. Finally, a PVD-GDC cell (red squares) show an OCV of around 1040 mV and a lower cell resistance than the SP-cells.

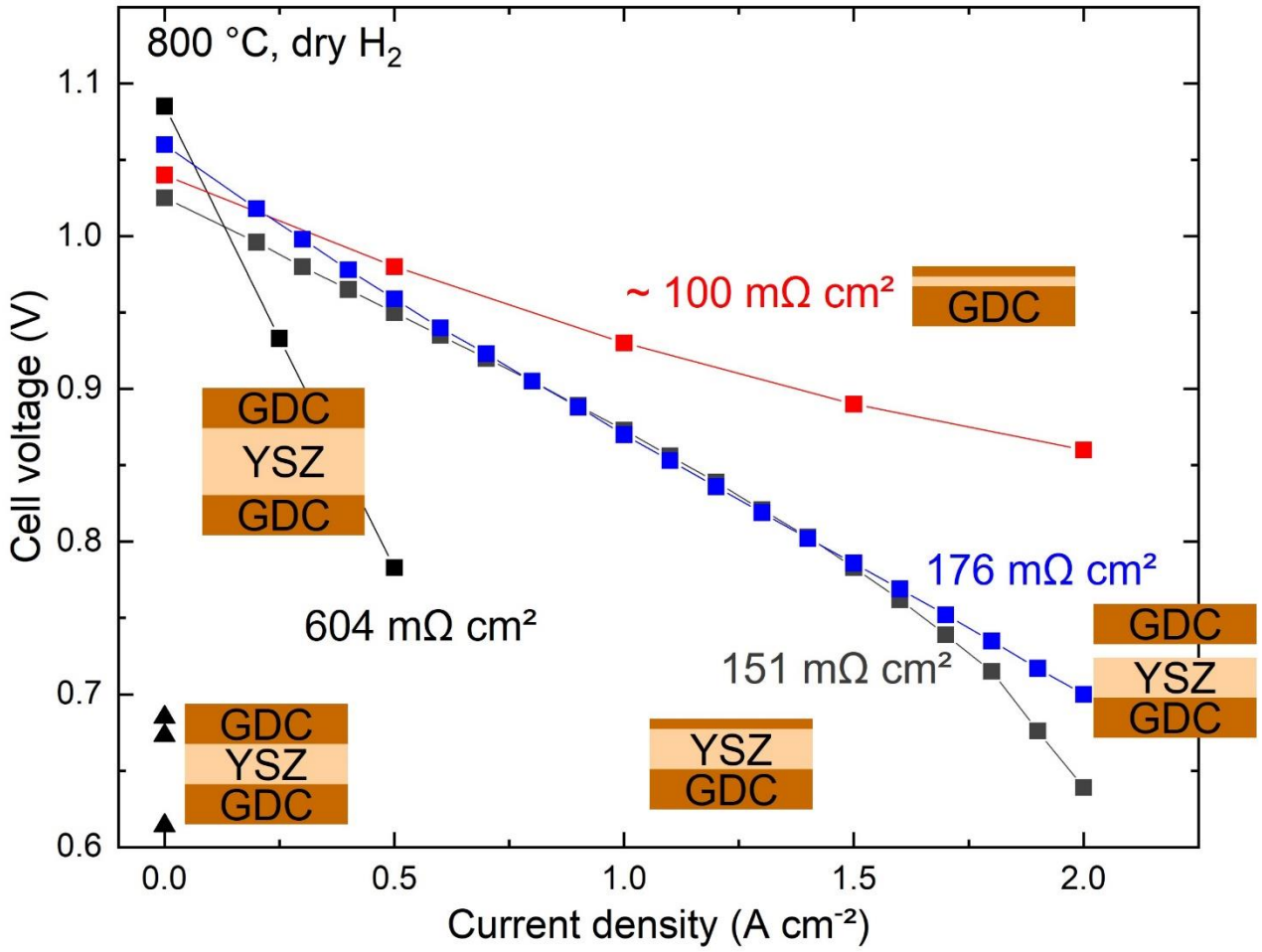

Figure 1: I-V curves for SP-cells with different geometries and a PVD-cell

An SP-cell with a bilayer electrolyte with approx. 12 µm of YSZ and a PVD cell were chosen for in-depth electrochemical characterization. The current-voltage curves recorded at temperatures of 700, 750 and 800 °C are shown in Figure 2. The I-V curves of the PVD cell was measured at 78.4% H_2O, while those of the SP-cell were measured between 78.4% and 20%, as indicated in the legend. The OCV of the PVD-cell is 0.876 V, which is slightly below the Nernst voltage for these conditions of V_N = 0.896 V. The deviation is likely due to leakage currents through the electrolyte, presumably mediated by defects in the GDC layer where the YSZ layer does not prevent electronic leakage. In contrast, the SP-cell shows an OCV equal to V_N at all temperatures and fuel compositions.

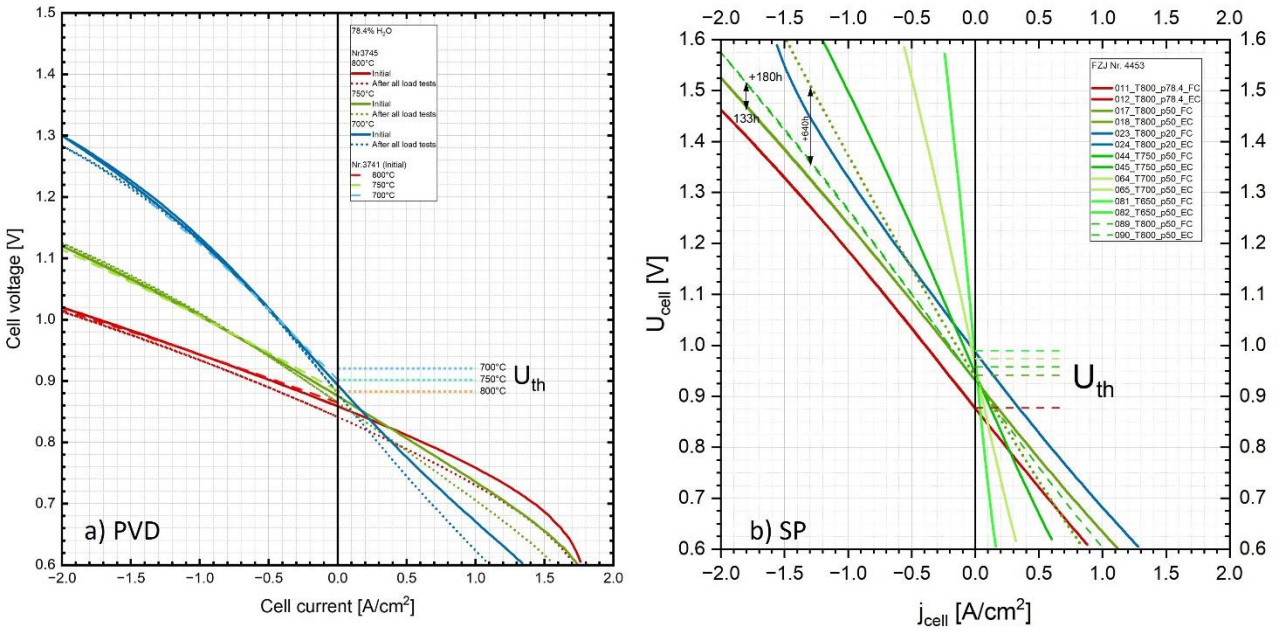

Figure 2: I-V curves of a PVD-cell (a)) and a SP-cell (b)) at various temperatures and humidity levels

The (apparent) performance of the PVD-cells is much better than of the SP-cells. At an electrolysis current of – 2 Acm^{-2}, the cell voltage is barely above 1 V. It should be pointed out that due to the leakage currents through the electrolyte, the Faradaic efficiency (FE) is likely below 1 and the measured current density does not correspond to the electrochemical reaction alone, but also to direct electronic leakage. In particular, the curvature of the I-V curve at high electrolysis current at 700 °C indicates a diminishing cell resistance with higher currents, indicative of the reduction of ceria and a correspondingly higher leakage current. This issue will be addressed in future work.
The performance of the PVD-cells is much lower, but the high OCV indicates that there are no leakage currents in these cells.

Single cell durability tests comparing the degradation over a period of > 500 hours are shown in Figure 3. The reference cells utilizing the state-of-the-art Ni-YSZ cathode show strong initial degradation during the 500 h period, with the voltage stabilizing after a few hundred hours. After 500 hours, the area-specific resistance (ASR) has increased from 193 $m\Omega cm^2$ to 306 $m\Omega cm^2$. Under the same testing conditions, the ASR of the PVD cell shows a small initial decrease and is then stable around 86 $m\Omega cm^2$ for almost 2000 hours. However, it is important to consider that the OCV of the PVD-cells is slowly but constantly falling during the test period, indicating increasing gas leakage and therefore a decrease in FE. Notably, the OCV shows a decrease of about 15 mV during the same time period.

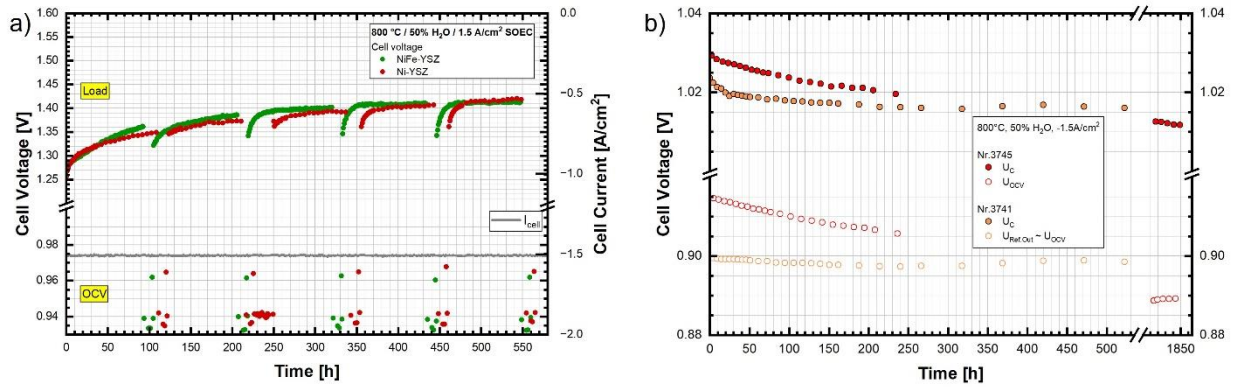

Figure 3: Degradation in SOEC operation at 800 °C, 50:50 H_2O:H_2 and 1.5 Acm^{-2}. A) Ni- and Ni(Fe)-YSZ reference; b) PVD cells.

The electrochemical testing of the SP-cells over 500 °C under identical conditions is shown in Figure 4 a) as voltage over time and b) ASR over time. The SP-cell shows a strong but decreasing degradation over the entire test period. Due to the high initial cell resistance of approximately 400 $m\Omega cm^2$, the cell voltage at the start of the test is above 1.5 V. After 500 hours, ASR has increased to approx. 475 $m\Omega cm^2$, corresponding to a cell voltage of 1.63 V. Even though the electrolysis voltage is higher than that of the Ni-YSZ reference cell, the voltage increase is slightly lower. Notably, the polarization resistance increases for about 200 hours and the remains constant, while the ohmic resistance shows a steady increase for the whole test duration.

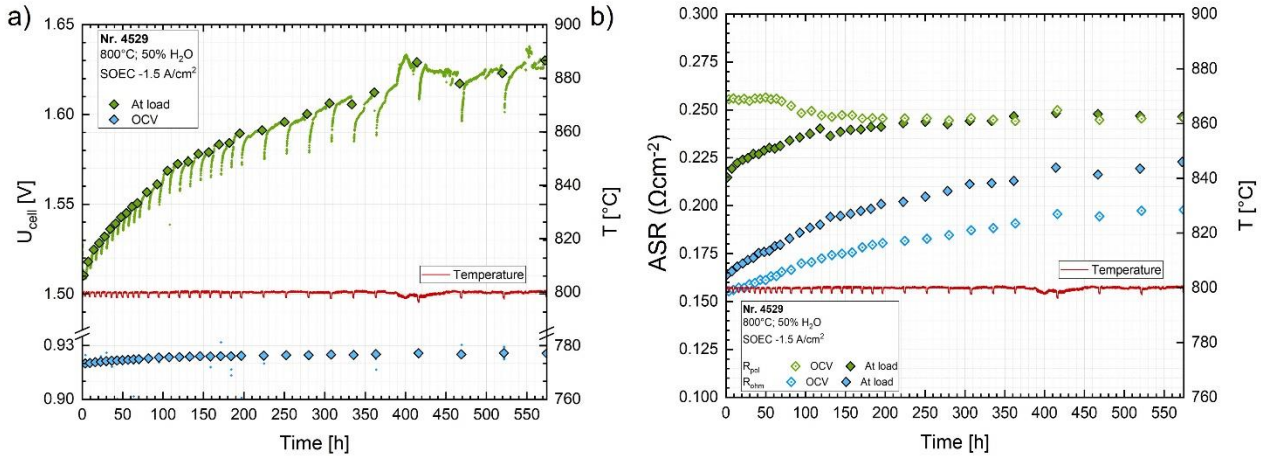

Figure 4: Degradation of the SP-cell in SOEC operation at 800 °C, 50:50 H_2O:H_2 and 1.5 Acm^{-2}.

After electrochemical testing, the microstructure of the PVD- and SP-cells was analyzed. 3D reconstructions of the Ni-GDC fuel electrode were performed via FIB-SEM to investigate possible Ni migration in the PVD cell during the harsh degradation test. The resulting reconstructions are shown in Figure 5 a) for testing duration of 0 h (reference), 1100 h and 2000 h. The microstructural parameters extracted from these are listed in Table 1. Within the expected standard deviations, the microstructural parameters extracted do not show a systematic trend with operation time. There is no indication of Ni migration taking place, either in the extracted numerical values nor in the images themselves. As shown in the cross-section after 2000 hours in Figure 5 b), the Ni remains well-dispersed in the fuel electrode.

The most notably feature of the cross-sections are cracks in the active layers of the cell. These cracks are not singular features, but appear regularly and are thus indicative of mechanical stresses affecting the entire cell. While such cracks could be a result of stresses developing during cooling, the continuously falling OCV of the cell during the electrolysis test suggests that these cracks form during cell testing already. The effect of electro-chemo-mechanical expansion in these cells has been analyzed in terms of elastic stresses, and the expansion of the dense GDC layer was found to produce high compressive stresses in this layer.[12] However, the cracks found after testing indicate tensile stresses normal to the electrolyte plane and resemble cracks caused by fuel electrode reoxidation (for which there is no sign). Investigations into the mechanism of cracking are ongoing.

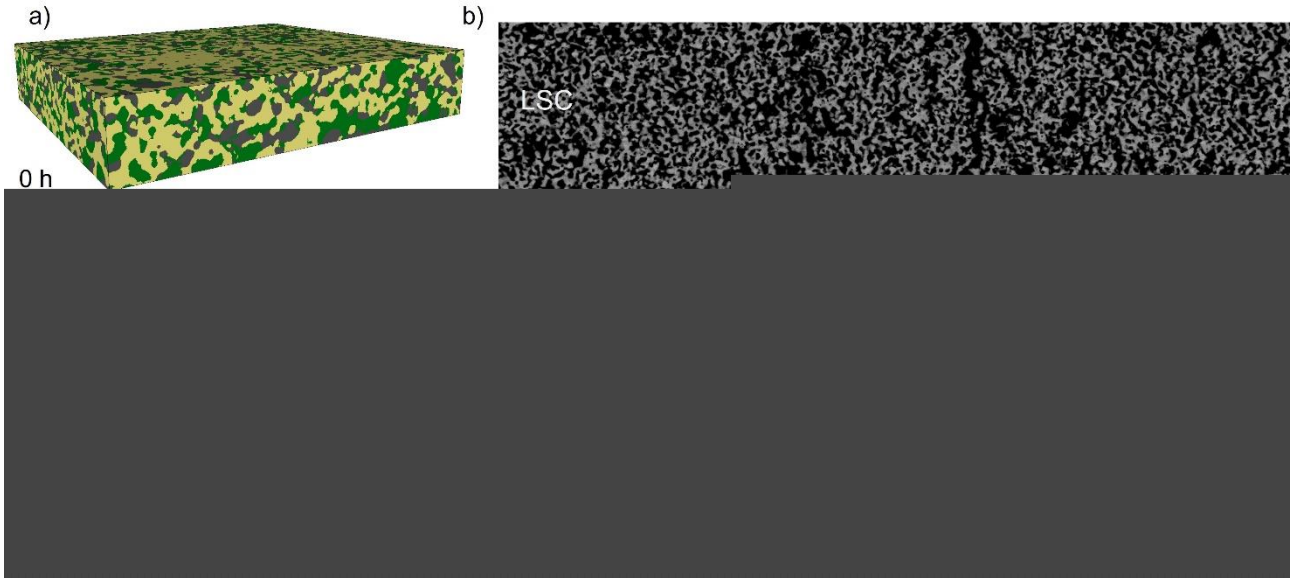

Figure 5: post-test analysis of the PVD cell. a) FIB-SEM reconstructions of an untested cell (0h), and two cells after 1100 h and 2000 h of testing. b) Representative SEM image of the cell cross-section after 2000 h of testing.

Table 1: Microstructural parameter of three PVD cells

Microstructural parameter	Material	0 h	1100 h	2000 h
Volume fraction FE (%)	CGO	49	51	50
	Pores	22	21	21
	Ni	29	28	29
Tortuosity	Pores (FE)	4.9	4.5	4.4
	Ni	4.5	5.7	4.8
Area/Volume (μm^{-1})	Ni	0.01	0.009	0.01
TPB/VolElectrode (μm^{-1})		0.04	0.08	0.05

Figure 6 a) shows SEM images of the microstructure of an SP cell after reduction of the cell, and b) shows a similar cell after 500 hours of electrolysis testing. Both GDC and YSZ layer show a thickness of approximately 12 µm. But the increased thickness of electrolyte layers

is not a sufficient explanation of the high ohmic resistance of the cell. While both GDC and YSZ are well densified, there is a highly porous region located at the interface between the two layers. These pores are likely the result of a Kirkendall effect due to dissimilar diffusion coefficients, but also likely a result of the directional forces present in the layers during densification. Any mismatch in densification kinetics would produce a force at the interface acting on the neighboring layer, and the formation of a pore network alleviates the stress associated to this mismatch. The interface likely limits the cell performance in two ways: the high porosity reduces the effective area of the cell, and a YSZ-GDC mixed phase is formed in the contact points which shows lower conductivity than either parent compound.[3,4]

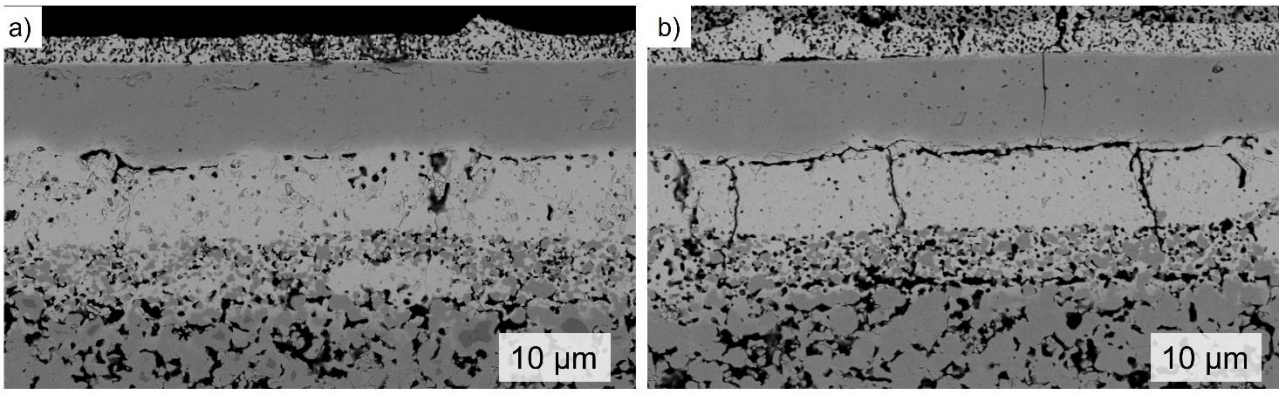

Figure 6: SEM micrographs of polished cross-section of a) a cell before and b) after 500 h of electrolysis testing.

The tested cell in Figure 6 b) shows several major effects that likely affect cell performance. There is some indication of delamination of the GDC barrier layer underneath the LSC air electrode, which could be a result of the high overpotential. However, it is also possible that this is a result of the manufacturing. More strikingly, the porous interface between the GDC and YSZ layer shows extensive cracking along the interface. The two layers seem detached in large sections of the cell. The most likely explanation is that the electro-chemo-mechanical expansion of the GDC layer produces shear stresses at the few contact points that connect the two layers mechanically. Since the YSZ layer does not expand, these stresses could lead to mechanical failure at the contact points. This is in agreement with the steady increase of ohmic resistance, which could be due to a continuous loss of contact between the two layers.

The GDC layer also shows extensive cracking perpendicular to the electrolyte plane. These cracks do not continue in the YSZ layer, which is likely why the OCV does not deteriorate. It seems intuitive that these cracks have the same origin as the cracks in the GDC electrolyte of the PVD cell. The SP cell has a much higher density of cracks than the PVD cell, which is likely due to the much higher cell voltage and an accordingly larger expansion of the GDC layer. However, the formation mechanism of these cracks in not understood and remains under investigation.

References

1. Kerafol GmbH, Datenblatt KeraCell III. (2015).
2. Leah, R., Bone, A., Hjalmarsson, P., et al., Commercialization of Ceres SteelCell® Technology for Power Generation and Electrolysis. ECS Transactions (2023);111:121.
3. Lenser, C., Jeong, H., Sohn, Y. J., et al., Interaction of a ceria-based anode functional layer with a stabilized zirconia electrolyte: considerations from a materials perspective. Journal of the American Ceramic Society (2017);101:739-48.

4. Tsoga, A., Naoumidis, A., and Stöver, D., Total electrical conductivity and defect structure of ZrO2–CeO2–Y2O3–Gd2O3 solid solutions. Solid State Ionics (2000);135:403-09.
5. Schwiers, A., Lenser, C., Guillon, O., et al., Interdiffusion at electrochemical interfaces between yttria-stabilized zirconia and doped ceria. Journal of the European Ceramic Society (2023);43:6189-99.
6. Klitkou, M. P., Lopez de Moragas, A., Taubmann, J., et al., Investigating viability of low temperature co-sintering to produce Ni-YSZ supported solid oxide electrolysis cells with a Ni-GDC active layer. Applied Energy (2025);400:126547.
7. Zhang, J., Lenser, C., Russner, N., et al., Boosting intermediate temperature performance of solid oxide fuel cells via a tri-layer ceria–zirconia–ceria electrolyte. Journal of the American Ceramic Society (2022);106:93-99.
8. Robinson, I. A., Huang, Y. L., Horlick, S. A., et al., Mitigating Electronic Conduction in Ceria-Based Electrolytes via External Structure Design. Advanced Functional Materials (2024);34.
9. Lopez de Moragas, A., Yarahmadi, M., Phan Klitkou, M., et al., Impact of Ni-GDC fuel electrode microstructure on cell performance in fuel electrode-supported solid oxide cells. Journal of Power Sources (2026);676:239854.
10. Schöller, L., Wehner, L., Ramler, D., et al., Understanding electro-chemo-mechanical stresses in ceria-based solid oxide electrolysis cells using virtual microstructures. under review.
11. Schafbauer, W., Menzler, N. H., and Buchkremer, H. P., Tape Casting of Anode Supports for Solid Oxide Fuel Cells at Forschungszentrum Jülich. International Journal of Applied Ceramic Technology (2014);11:125-35.
12. Lenser, C., Zhang, J., Russner, N., et al., Electro-chemo-mechanical analysis of a solid oxide cell based on doped ceria. Journal of Power Sources (2022);541:231505.

Keywords: EFCF2026, SOC, Electrolysers, SOE, Ceria, Electro-chemo-mechanics, degradation, Ni migration